

Photophysical and Novel Charge-Transfer Properties of Adducts between $[\text{Ru}^{\text{II}}(\text{bpy})_3]^{2+}$ and $[\text{S}_2\text{Mo}_{18}\text{O}_{62}]^{4-}$

Tia E. Keyes,^{*,†} Etienne Gicquel,[‡] Liz Guerin,[‡] Robert J. Forster,[†] Victoria Hultgren,[§] Alan M. Bond,[§] and Anthony G. Wedd^{||}

School of Chemical Sciences, Dublin City University, Glasnevin, Dublin 9, Ireland, School of Chemistry, Dublin Institute of Technology, Kevin St., Dublin 8, Ireland, Department of Chemistry, Monash University, PO Box 23, Victoria 3800, Australia, and School of Chemistry, University of Melbourne, Victoria 3010, Australia

Received November 20, 2002

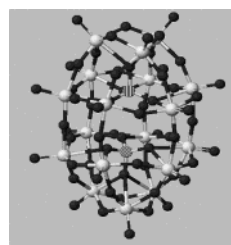
The photophysical properties of acetonitrile solutions of $[\text{Ru}(\text{bpy})_3]^{2+}$ and $[\text{S}_2\text{Mo}_{18}\text{O}_{62}]^{4-}$ are described. We discuss evidence for ion cluster formation in solution and the observation that despite the strong donor ability of the excited state of $[\text{Ru}(\text{bpy})_3]^{2+}$ and its inherent photolability, adducts with $[\text{S}_2\text{Mo}_{18}\text{O}_{62}]^{4-}$ were photostable. Photophysical studies suggest that the quenching of the $[\text{Ru}(\text{bpy})_3]^{2+}$ excited state by $[\text{S}_2\text{Mo}_{18}\text{O}_{62}]^{4-}$ occurs via a static mechanism and that binding is largely electrostatic in nature. Evidence is provided from difference spectroscopy and luminescence excitation spectroscopy for good electronic communication between $[\text{Ru}(\text{bpy})_3]^{2+}$ and $[\text{S}_2\text{Mo}_{18}\text{O}_{62}]^{4-}$ with the presence of a novel, luminescent, inter-ion charge-transfer transition. The identity of the transition is confirmed by resonance Raman spectroscopy.

Introduction

Heteropolyoxomolybdate anions exhibit remarkably rich redox and photochemistry, as a consequence of their ability to act as electron and oxygen relays. These properties have lead to their increasing industrial and medical importance.¹ Particular applications include photooxidation and photocatalysis,² as well as development of efficient catalysts for selective oxidation of organic compounds in mild and environmentally friendly conditions.³

The Dawson anions $\alpha\text{-}[\text{S}_2\text{Mo}_{18}\text{O}_{62}]^{4-}$, structure 1, and $\alpha\text{-}[\text{S}_2\text{Mo}_{18}\text{O}_{62}]^{5-}$ contain sulfur as the central heteroatoms. They may be activated photochemically through a ligand to metal charge-transfer transition to generate extremely powerful oxidants. Quantitative photoelectrochemical studies on these species in the presence of donors such as DMF and THF reveal a facile photooxidation of organics as difficult to oxidize as toluene.⁴ However, despite being a powerful

photooxidant, $[\text{S}_2\text{Mo}_{18}\text{O}_{62}]^{4-}$ is not greatly activated by visible light.



Structure 1

Thus, the development of a sensitized system in which a second metal complex could efficiently harvest an incident photon followed by the creation of a $[\text{S}_2\text{Mo}_{18}\text{O}_{62}]^{5-}$ -based excited state would be a significant advance in this field. $[\text{Ru}(\text{bpy})_3]^{2+}$ is an attractive candidate for this approach because of its intense visible absorbance and advantageous, well-understood photophysical properties.

Moreover, the capacity of multicharged cation complexes such as $[\text{Os}(\text{bpy})_3]^{2+}$ to electrostatically bind to polyoxomolybdate anions has been demonstrated by Anson et al.⁵

* To whom correspondence should be addressed. E-mail: tia.keyes@dcu.ie.

† Dublin City University.

‡ Dublin Institute of Technology.

§ Monash University.

|| University of Melbourne.

(1) Polyoxometalate Chemistry. In *Topology via Self-assembly to Applications*; Pope, M. T., Müller, A., Eds.; Kluwer Academic Publishers: Dordrecht, The Netherlands, 2001.

(2) Papaconstantinou, E. *Chem. Soc. Rev.* **1989**, 18, 1.

(3) Neumann, R. *Prog. Inorg. Chem.* **1998**, 47, 317.

(4) Bond, A. M.; Way, D. M.; Wedd, A. G.; Compton, R. G.; Booth, J.; Eklund, J. C. *Inorg. Chem.* **1995**, 34, 3378

(5) Kuhn, A.; Anson, F. C. *Langmuir* **1996**, 12, 5481.

Their observations were consistent with monolayers of $[\text{P}_2\text{Mo}_{18}\text{O}_{62}]^{6-}$ on electrode surfaces binding electrostatically to $[\text{Os}(\text{bpy})_3]^{2+}$ cations to create multilayers of alternating molybdate and osmium ions. Furthermore, the salt $[\text{Ru}(\text{bpy})_3]_2[\text{S}_2\text{Mo}_{18}\text{O}_{62}]$ was isolated recently by Hultgren et al.⁶ and shown to possess a rich redox chemistry in the solid state.⁷

In this contribution, we describe the photophysical properties of acetonitrile solutions of $[\text{Ru}(\text{bpy})_3]^{2+}$ and $[\text{S}_2\text{Mo}_{18}\text{O}_{62}]^{4-}$. We discuss evidence for ion cluster formation in solution and the observation that despite the strong donor ability of the excited state of $[\text{Ru}(\text{bpy})_3]^{2+}$ and its inherent photolability, adducts with $[\text{S}_2\text{Mo}_{18}\text{O}_{62}]^{4-}$ were photostable. Evidence is provided for good electronic communication between $[\text{Ru}(\text{bpy})_3]^{2+}$ and $[\text{S}_2\text{Mo}_{18}\text{O}_{62}]^{4-}$ and the presence of a novel luminescent inter-ion charge-transfer transition which is, to our knowledge, the only report of a luminescent inter-ion charge transfer transition of this nature involving $[\text{Ru}(\text{bpy})_3]^{2+}$. One other comparable study of the luminescence quenching ability of heteropolyoxometalates has been conducted. Ballardini et al. reported luminescence quenching studies of $[\text{Ru}(\text{bpy})_3]^{2+}$ by the substituted Keggin anion $[(\text{HO}-\text{Mn})\cdot\text{PW}_{11}\text{O}_{39}]^{6-}$.⁸ Both static and dynamic electron transfer processes were observed in solution, and electronic communication appears to be significantly less than observed in the present study.

The investigations presented here provide fundamental insights that may underlie photocatalytic development in this area.

Experimental Section

Materials. $[(\text{C}_6\text{H}_{13}\text{N})_4[\text{S}_2\text{Mo}_{18}\text{O}_{62}]]$ and $[\text{Ru}(\text{bpy})_3]\text{Cl}_2$ were synthesized according to published methods.^{7,9} HPLC grade acetonitrile, 99.9%, dried over molecular sieves, 3A, was employed for all photochemical studies. All other reagents, purchased from Sigma-Aldrich, were used as received.

Steady-state emission spectra were recorded employing a Perkin-Elmer LS50B luminescence spectrometer. Time-resolved luminescence studies were conducted with an Edinburgh Instruments F900 time-correlated single photon counting or a custom-built laser photolysis system. In the latter system, luminescent lifetimes were measured using the second (532 nm, 50 mJ/pulse) or third harmonic (355 nm, 30 mJ/pulse) of a Continuum Surelite Q-switched Nd:YAG laser for excitation. Emission was detected in a right-angled configuration to the laser using an Andor model M20 gated intensified CCD coupled to an Oriel model MS125 spectrograph. With suitable signal averaging, this configuration allows a complete emission spectrum (spectral range 250 nm) to be obtained within times as short as 10 ns. The emission spectra were typically recorded using the average of 10 laser shots. The gatewidth, i.e., the exposure time of the CCD, was never more than 5% of the excited state lifetime. The step size, i.e., the time between the acquisition of discrete spectra, was typically 5% of the excited state half-life.

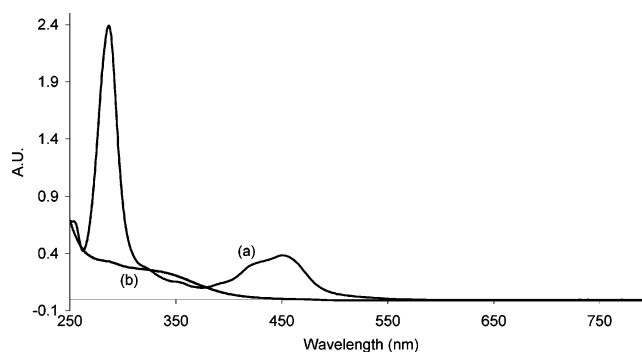


Figure 1. Electronic spectrum of (a) $[\text{Ru}(\text{bpy})_3]^{2+}$ and (b) of $[\text{S}_2\text{Mo}_{18}\text{O}_{62}]^{4-}$ in dry acetonitrile.

Time-resolved absorption spectra were collected using the same instrumentation in absorption mode with an Oriel 300 W Xe arc lamp acting as the monitoring source. In this instance, spectra were typically recorded using the average of 25 laser shots. The gate width, i.e., the exposure time of the CCD, was never more than 10% of the excited-state lifetime.

Absorption spectra were measured using a Shimadzu 3100 UV-vis/NIR spectrophotometer.

Raman spectroscopy was conducted on a Dilor Jobinyvon Spex Labram. The exciting Arion laser (514, 488, or 457.9 nm) was focused into the cell or onto a solid sample using a 10 \times objective lens. A spectral resolution of 1.5 cm^{-1} /pixel was achieved using a grating of 1800 lines/mm, and the x -axis was calibrated against acetonitrile.

Computations, such as spectral fitting and extraction of lifetime data, were conducted using standard iterative techniques on Microsoft Excel.¹⁰

Results and Discussion

Luminescence Studies. Figure 1 shows the electronic spectroscopy of $[\text{Ru}(\text{bpy})_3]^{2+}$ and $[\text{S}_2\text{Mo}_{18}\text{O}_{62}]^{4-}$; $[\text{Ru}(\text{bpy})_3]^{2+}$ possesses a strong visible absorbance centered at 452 nm and well-characterized luminescence behavior with a λ_{max} centered at 600 nm. λ_{max} for $[\text{S}_2\text{Mo}_{18}\text{O}_{62}]^{4-}$ is centered around 350 nm with no visible absorbance and no discernible luminescence. The $[\text{Ru}(\text{bpy})_3]^{2+}$ emission provides a sensitive means of interrogating the interactions between this complex and $[\text{S}_2\text{Mo}_{18}\text{O}_{62}]^{4-}$, whereby, for example, electron or energy transfer interactions may be manifested by decreasing emission intensity. The combined concentrations of these cations and anions were maintained below 6×10^{-4} M due to the relatively low solubility of the 2:1 salt $[\text{Ru}(\text{bpy})_3]_2[\text{S}_2\text{Mo}_{18}\text{O}_{62}]$ in acetonitrile. Above this concentration, the solutions become turbid.

Figure 2 illustrates the impact of addition of $[\text{S}_2\text{Mo}_{18}\text{O}_{62}]^{4-}$, up to 1×10^{-4} M, on the luminescence spectrum of $[\text{Ru}(\text{bpy})_3]^{2+}$. The spectra were excited at 450 nm, and the $[\text{Ru}(\text{bpy})_3]^{2+}$ concentration was maintained at 1.0×10^{-5} M in acetonitrile. The luminescence intensity decreased progressively with increasing concentrations of $[\text{S}_2\text{Mo}_{18}\text{O}_{62}]^{4-}$. Over the anion concentration range (0–4.0) $\times 10^{-6}$ M isoemissive points were maintained at 549 and 696 nm but were lost at higher anion concentrations.

(6) Hultgren, V. M.; Bond, A. M.; Wedd, A. G. *J. Chem. Soc., Dalton Trans.* **2001**, 1076.

(7) Cooper, J. B.; Way, D. M.; Bond, A. M.; Wedd, A. G. *Inorg. Chem.* **1993**, *32*, 2416.

(8) Ballardini, R.; Gandolfi, M. T.; Balzani, V. *Inorg. Chem.* **1987**, *26*, 862.

(9) Palmer, R. A.; Piper, T. S. *Inorg. Chem.* **1966**, *5*, 864.

(10) Diamond, D.; Hanratty, V. *Excel for Chemists*; John Wiley & Sons, VCH: New York, 1997.

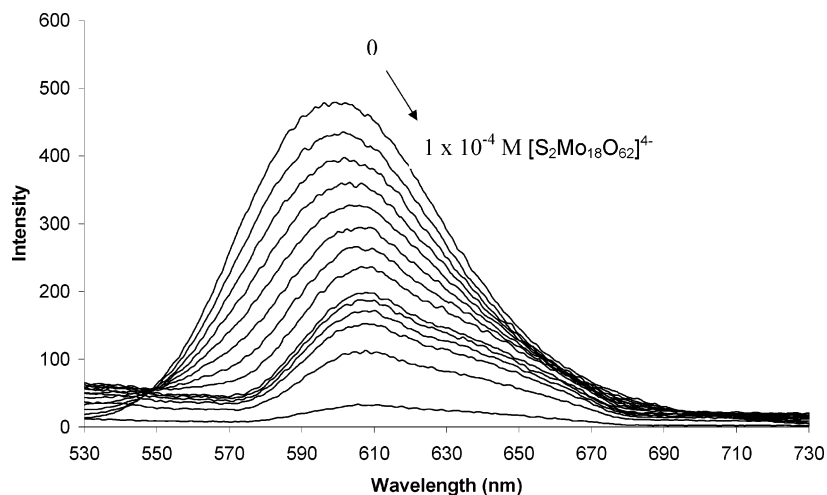


Figure 2. Emission spectrum (uncorrected) in dry acetonitrile of $[\text{Ru}(\text{bpy})_3]^{2+}$ (1×10^{-5} M) on addition of $[\text{S}_2\text{Mo}_{18}\text{O}_{62}]^{4-}$ (excitation wavelength 450 nm).

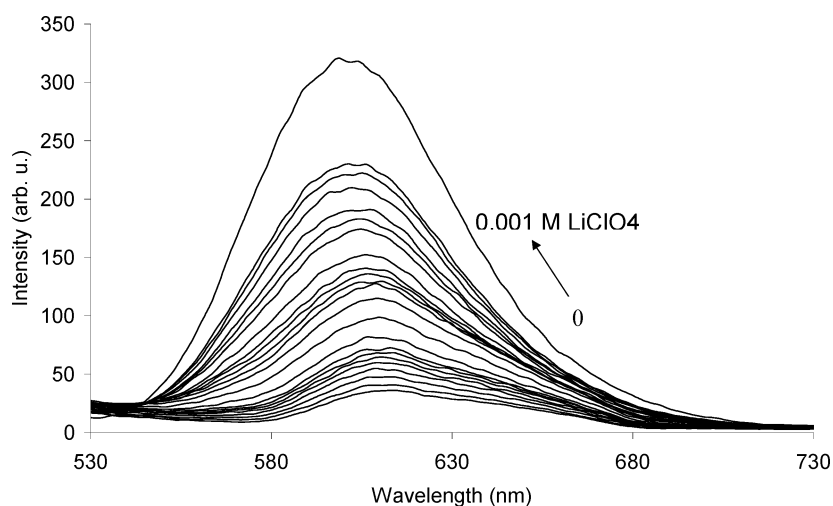


Figure 3. Emission spectrum (uncorrected) of an acetonitrile solution of $[\text{Ru}(\text{bpy})_3]^{2+}$ (1×10^{-5} M) and $[\text{S}_2\text{Mo}_{18}\text{O}_{62}]^{4-}$ (1×10^{-4} M), corresponding primarily to the formation of 1:1 complex, initially in natural ionic strength solution and then after addition of aliquots of LiClO_4 in dry acetonitrile (excitation wavelength 450 nm).

In addition to these changes to luminescence intensity, significant changes in the $[\text{Ru}(\text{bpy})_3]^{2+}$ $^3\text{MLCT}$ emission maximum occurred on addition of $[\text{S}_2\text{Mo}_{18}\text{O}_{62}]^{4-}$. In the higher cation:anion ratio range, up to 10:1, a red shift from 600 to 612 nm in λ_{max} was observed with a decrease in quantum yield of about 50%. At lower ratios, a second band appeared as a shoulder on the emission profile. Spectral fitting indicated that this feature was centered at 640 nm, its appearance commencing at a cation:anion ratio of about 3:1.

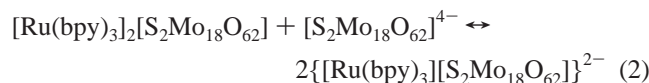
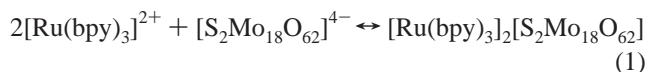
In quenching studies of $[\text{Ru}(\text{bpy})_3]^{2+}$ by the substituted Keggin anion $[(\text{HO}-\text{Mn})\cdot\text{PW}_{11}\text{O}_{39}]^{6-}$, red shifts of less than 4 nm were reported.⁷ The shifts in the emission maximum on addition of $[\text{S}_2\text{Mo}_{18}\text{O}_{62}]^{4-}$ in the present system are considerably larger. In addition, the luminescence intensity at a cation:anion ratio of 1:3 decreased to about 10% of that of free $[\text{Ru}(\text{bpy})_3]^{2+}$ in solution. This behavior could be due to a strong dynamic quenching at such high relative anion concentrations, but the evidence presented below favors an associated or static quenching mechanism.

To probe the possibility of static quenching due to ion cluster formation, the ionic strength was varied. Lithium perchlorate or tetrabutylammonium tetrafluoroborate salts

were employed to control the ionic strength in acetonitrile, as they dissociate completely in this high dielectric solvent.¹¹ Figure 3 presents luminescence spectra for solutions containing $[\text{Ru}(\text{bpy})_3]^{2+}$ (1×10^{-5} M) and added aliquots of $[\text{S}_2\text{Mo}_{18}\text{O}_{62}]^{4-}$ up to a concentration of 1×10^{-4} M, corresponding to a cation:anion ratio of 1:10. The initial spectrum of relatively low intensity was equivalent to the final spectrum of Figure 2. Addition of LiClO_4 resulted in increasing luminescence intensity, and the limiting spectrum at concentrations of salt in excess of 0.08 M was indistinguishable from that of free $[\text{Ru}(\text{bpy})_3]^{2+}$ in acetonitrile. It was necessary to add NBu_4BF_4 to a concentration of 0.1 M to obtain the same limiting spectrum. Control experiments in the absence of $[\text{S}_2\text{Mo}_{18}\text{O}_{62}]^{4-}$ showed that addition of either salt to a concentration of 0.1 M had no impact on either λ_{max} or the quantum yield of the $[\text{Ru}(\text{bpy})_3]^{2+}$ luminescence. These results indicate that interactions between $[\text{Ru}(\text{bpy})_3]^{2+}$ and $[\text{S}_2\text{Mo}_{18}\text{O}_{62}]^{4-}$ are predominantly electrostatic in nature and that ion pairing can be disrupted by addition of salt.

(11) Bard, A. J.; Faulkner, L. R. *Electrochemical Methods, Fundamentals and Applications*, 2nd ed.; J. Wiley and Sons: New York, 2001.

Figure 2 reveals that an isoemissive point is absent over the entire range of $[\text{S}_2\text{Mo}_{18}\text{O}_{62}]^{4-}$ additions, which indicates the formation of intermediates, possibly through a two-step association process. The following equilibria are likely to be present in solution, and as shown below, this model provides a consistent interpretation of the spectroscopic data:



As $[\text{Ru}(\text{bpy})_3]^{2+}$ is the luminescent species, the experiments involve addition of $[\text{S}_2\text{Mo}_{18}\text{O}_{62}]^{4-}$ as the quencher to a solution of $1 \times 10^{-5} \text{ M}$ $[\text{Ru}(\text{bpy})_3]\text{Cl}_2$. Since $[\text{Ru}(\text{bpy})_3]\text{Cl}_2$ is in excess in the initial stages of the titration, the 2:1 ion cluster $[\text{Ru}(\text{bpy})_3]_2[\text{S}_2\text{Mo}_{18}\text{O}_{62}]$ is proposed to form initially, and indeed this cluster has been isolated previously,⁶ followed by formation of the 1:1 ion pair when the polyoxomolybdate anion is present in large excess.

The studies presented here were conducted in aerated solution. Deaeration had essentially no impact on the relative extent of quenching of $[\text{Ru}(\text{bpy})_3]^{2+}$ by $[\text{S}_2\text{Mo}_{18}\text{O}_{62}]^{4-}$, reflected in the slopes of the Stern–Volmer plots, which were independent of the presence of O_2 in the analyte solutions.

Excitation Spectra. To investigate the origin of the luminescence changes illustrated in Figures 2 and 3, excitation spectra were collected at various cation:anion ratios with the detector set to 590 and 650 nm. An excitation spectrum is a plot of the emission intensity versus the excitation wavelength. Typically, it is similar to an absorbance spectrum but only the absorbances responsible for emission are recorded. These wavelengths corresponded closely with the two λ_{max} values observed in the luminescence spectra but were chosen so as to minimize the contribution from the adjacent band to the excitation curve.

The excitation spectra for 590 and 650 nm were recorded over the same concentration range as for the emission titration. A possible origin of the shoulder at 640 nm is Jahn–Teller distortion of the $[\text{Ru}(\text{bpy})_3]^{2+}$ complex which may be enhanced by binding to $[\text{S}_2\text{Mo}_{18}\text{O}_{62}]^{4-}$. This can be manifested as vibronic fine structure observed as a shoulder on the luminescence spectrum.¹² However, Figure 4 shows, rather surprisingly, that the two emission bands have different origins. Detecting for emission at 590 nm, the excitation spectrum, Figure 4a, is reminiscent of the absorbance spectrum for $[\text{Ru}(\text{bpy})_3]^{2+}$ with a λ_{max} centered around 450 nm.¹³ With monitoring at 590 nm during the addition of anion, two isosbestic points at 364 and 409 nm were observed, and these were maintained over the entire $[\text{S}_2\text{Mo}_{18}\text{O}_{62}]^{4-}$ concentration range.

Figure 4b illustrates the excitation spectrum obtained detecting for emission at 650 nm. This spectrum is remark-

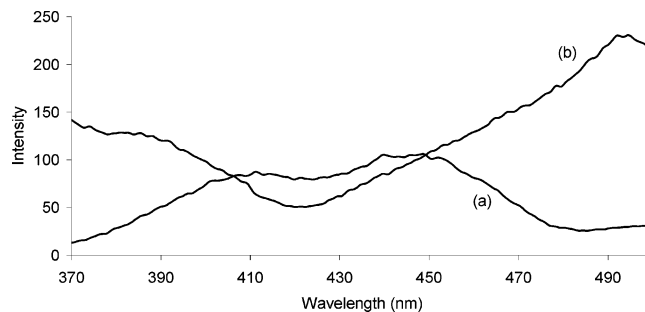


Figure 4. Uncorrected excitation spectra in dry acetonitrile for $[\text{Ru}(\text{bpy})_3]^{2+}$ and $(1 \times 10^{-5} \text{ M}) [\text{S}_2\text{Mo}_{18}\text{O}_{62}]^{4-}$ with detecting at (a) 590 nm and (b) 650 nm.

ably different from that observed in Figure 4a. The band characteristic of $[\text{Ru}(\text{bpy})_3]^{2+}$ at 450 nm disappears upon progressive addition of anion, and a broad band centered at 485 nm grows in. This new absorbance feature is certainly not due to free $[\text{S}_2\text{Mo}_{18}\text{O}_{62}]^{4-}$, which is nonemissive and absorbs in the near-UV region as shown in Figure 1.^{3,7} As the $[\text{S}_2\text{Mo}_{18}\text{O}_{62}]^{4-}$ concentration was increased, isosbestic points were maintained at 406 nm and 462 nm in this excitation spectrum. As the band at 450 nm reduced in intensity, the new feature at 485 nm increased in intensity.

At high anion concentrations ($>4 \times 10^{-5} \text{ M}$), the intensity of this new transition decreased. This is attributed to the gradual loss of luminescence of the complex responsible for the excitation spectrum rather than genuine loss of this absorbance feature.

The excitation spectra shown in Figure 4 confirms that there are at least two emitting species in solution. As described previously, the absence of an isoemission point in the emission spectra suggested that an intermediate species is present. Detection of the emission at wavelengths where the contribution from the second species is low relative to the target species allowed the two emitting species to be monitored somewhat independently. This accounts for the fact that isosbestic points are maintained in the excitation spectra over the entire anion concentration range, since the $[\text{Ru}(\text{bpy})_3]^{2+}$ and cluster complexes can be observed reasonably independently in this way. The observations are consistent with the presence of the two product species, $[\text{Ru}(\text{bpy})_3]_2[\text{S}_2\text{Mo}_{18}\text{O}_{62}]$ and $\{[\text{Ru}(\text{bpy})_3][\text{S}_2\text{Mo}_{18}\text{O}_{62}]\}^{2-}$, of eqs 1 and 2.

Since $[\text{Ru}(\text{bpy})_3]^{2+}$ is the emitting species and $[\text{S}_2\text{Mo}_{18}\text{O}_{62}]^{4-}$ exhibits no luminescence, titrations must be conducted through the addition of the quenching $[\text{S}_2\text{Mo}_{18}\text{O}_{62}]^{4-}$ species to the $[\text{Ru}(\text{bpy})_3]^{2+}$ solution. Consequently, the 2:1 ion cluster would tend to form first, at initially high cation:anion ratio, consistent with the 2:1 product isolated by Hultgren et al.⁶ The 1:1 ion pair would be favored as the titration continued, and it is this species that we tentatively propose to be the source of the luminescence at 640 nm, since this emission shoulder only appears in the luminescence spectrum at lower cation:anion ratios.

Time-Resolved Emission Spectroscopy and the Quenching Mechanism. Static and dynamic behavior in luminescence quenching can be distinguished by comparing the

(12) Lever, A. B. P. *Inorganic Electronic Spectroscopy*, 2nd ed.; Elsevier: New York, 1986.

(13) Juris, A.; Balzani, V.; Barigelletti, F.; Campagna, S.; Belser, P.; von Zelewsky, A. *Coord. Chem. Rev.* **1988**, *84*, 85.

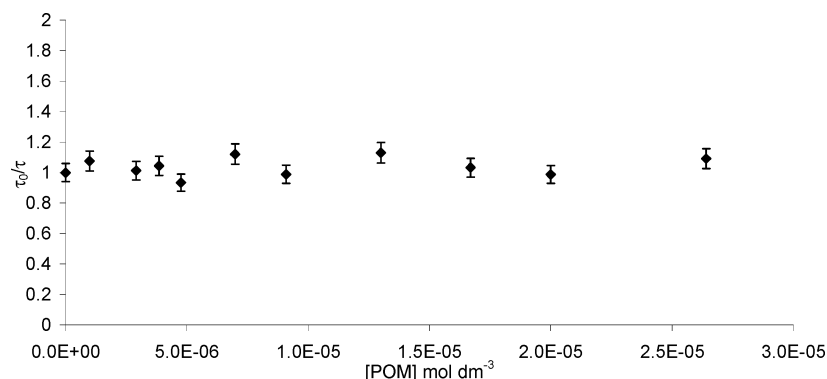


Figure 5. Stern–Volmer plot of the decay lifetime, τ , of photoexcited $[\text{Ru}(\text{bpy})_3]^{2+}$ (1×10^{-5} M) quenched by $[\text{S}_2\text{Mo}_{18}\text{O}_{62}]^{4-}$ in dry acetonitrile solution.

impact of quenching on steady-state luminescence intensity and on the luminescent lifetimes of the luminophore species.

In the absence of static association between the luminescent species and quencher, the luminescence quenching data are expected to follow the Stern–Volmer relation,

$$\frac{I_0}{I} \text{ or } \frac{\tau_0}{\tau} \text{ or } \frac{\phi_0}{\phi} = 1 + k_q \tau_0 [\text{Q}] \quad (3)$$

where I_0 and I are the luminescence intensities in the absence and presence of quencher, respectively, and τ , τ_0 and ϕ , ϕ_0 are the respective equivalent excited-state lifetimes and luminescence quantum yields. If the quenching process is dynamic, the slopes of I_0/I , ϕ_0/ϕ , or τ_0/τ plots versus quencher concentration $[\text{Q}]$ would be the same and equal to the product of the quenching rate constant, k_q , and the lifetime, τ_0 , of the luminescent species in the absence of quencher.

If the quenching mechanism is static, the model applied depends on the nature of the association between luminophore and quencher.¹⁴ However, as long as the mechanism is purely static, the luminescent lifetime should not be affected by quenching of the luminophore. Consequently, plots of I_0/I and τ_0/τ vs $[\text{Q}]$ will be very different.

Under circumstances where a ground-state association complex (e.g., ion pair) is formed between luminophore and quencher, the concentration dependence of luminescence intensity or quantum yields can be described by a model reminiscent of the Stern–Volmer model:

$$\frac{I_0}{I} \text{ or } \frac{\phi_0}{\phi} = 1 + K_{\text{ass}} [\text{Q}] \quad (4)$$

Here K_{ass} is the stability constant of the ground-state complex.

To assess the nature of the quenching in the present system, Stern–Volmer plots of luminescent lifetime and emission intensities for $[\text{Ru}(\text{bpy})_3]^{2+}$ and $[\text{S}_2\text{Mo}_{18}\text{O}_{62}]^{4-}$ were compared. Figure 5 shows a Stern–Volmer plot of the luminescent lifetime of $[\text{Ru}(\text{bpy})_3]^{2+}$ quenched by $[\text{S}_2\text{Mo}_{18}\text{O}_{62}]^{4-}$ in aerated solution. Although the expected decrease in intensity of the luminescent signal on addition of anion was observed in the transient signals, the observed lifetime was essentially constant, within experimental error. This behavior is typical of static quenching in which a

ground-state complex forms between fluorophore and quencher. Any initial change in lifetime from free fluorophore may be due to the formation of a complex that is itself luminescent, with a lifetime different from that of the parent fluorophore.¹⁵

Static quenching is commonly accompanied by dynamic quenching as was apparent in the studies of Ballardini et al.,⁷ where a decrease in τ accompanied each addition of quencher $[(\text{HO}-\text{Mn})\cdot\text{PW}_{11}\text{O}_{39}]^{6-}$ to a solution of $[\text{Ru}(\text{bpy})_3]^{2+}$. However, the slope of the τ_0/τ and I_0/I Stern–Volmer plots were significantly different, indicating the presence, simultaneously, of both static and dynamic quenching. In the present case, the quenching process appears to be entirely static in nature, without any obvious dynamic component.

Luminescence kinetics were also investigated using single photon counting methods conducted over a range of time domains and cation:anion ratios. In each instance, single exponential decays of the luminescent lifetime were observed. There was no evidence for a second component with a lifetime of greater than 5 ns, which represents the experimental limit of our instrumentation.

Consistent with the low intensity of the emission at 640 nm, it appears that the 1:1 ion pair is luminescent but that the luminescent lifetime of this species is substantially decreased compared with that of the free fluorophore, i.e., less than a few nanoseconds. These lifetime studies at natural ionic strength were also conducted exciting the sample at both 532 and 355 nm, to exclude the possibility that exciting into $[\text{S}_2\text{Mo}_{18}\text{O}_{62}]^{4-}$ influences the outcome. The results were identical in each case.

To further investigate the nature of the interaction between luminophore and quencher, data were treated according to the association complex model (eq 4) as in Figure 6. It is apparent from fitting of the data to either of these models, that there are two distinct data regions.

Reasonable agreement between theory and experiment is observed for both models, with comparable regression coefficients of approximately 0.995 being obtained where

(15) One possibility is that the lifetime of the quenched component based on the 640 nm emission is not represented on this plot because it is too short. However, on the basis of our experimental limitations, this would imply that the rate of quenching exceeds diffusion control. This would then have also to occur by a static or associated complex mechanism.

(14) Valeur, B. *Molecular Fluorescence, Principles and Applications*; Wiley VCH: New York, 2002; pp 72–124.

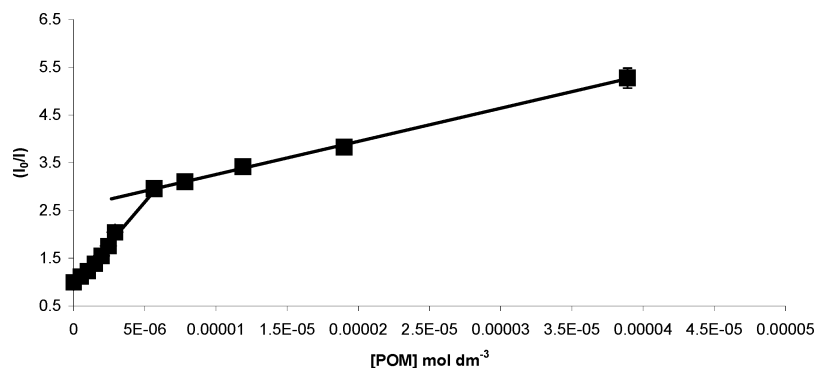


Figure 6. Static association plot of steady-state quenching of luminescence of $[\text{Ru}(\text{bpy})_3]^{2+}$ (1×10^{-5} M) by $[\text{S}_2\text{Mo}_{18}\text{O}_{62}]^{4-}$ in dry acetonitrile.

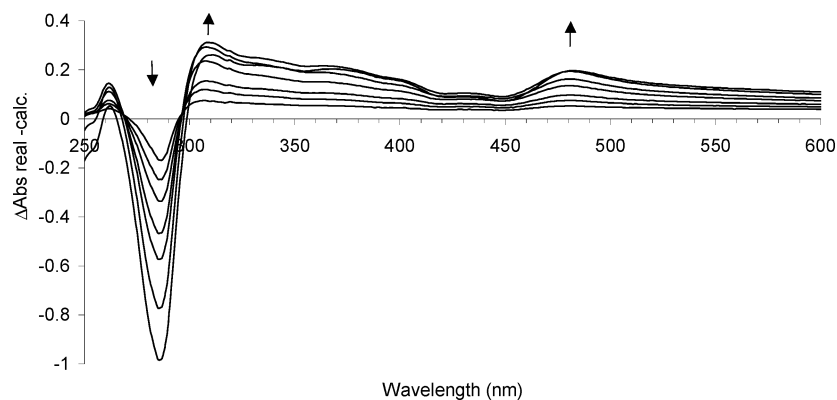


Figure 7. Difference UV-vis spectra (experimental - calculated) of the titration of $[\text{S}_2\text{Mo}_{18}\text{O}_{62}]^{4-}$ against $[\text{Ru}(\text{bpy})_3]^{2+}$ in dry acetonitrile.

fits are carried out over the two distinct data regions. The first linear region occurs between 0 and 4×10^{-6} M $[\text{S}_2\text{Mo}_{18}\text{O}_{62}]^{4-}$ (up to a cation:anion ratio of 3:1) and then between 4×10^{-6} and 1×10^{-4} M anion (up-to-a ratio of 1:10).

A combined static and dynamic model may also be applied to the data, but it is apparent from the lifetime data illustrated in Figure 3 that the quenching mechanism is purely static in nature. Any nonlinearity in the Stern-Volmer fits is attributed to the association complex being weakly emitting and to the fact that there are significant changes in the λ_{max} of emission throughout the titration. The association model for static quenching allows estimates of the equilibrium constant be made using eq 4. The association model (eqs 1 and 2) indicates that the first complex formed in the titration is the 2:1 ion cluster, corresponding to the first linear data region of Figure 6, followed by formation of the 1:1 ion pair. The association constants K_a for these ion pairs are estimated to be 4×10^5 and 3×10^4 , respectively.¹⁶

Electronic Spectroscopy. The emission and excitation spectra presented here suggested that new optical features may be present in solutions containing both $[\text{Ru}(\text{bpy})_3]^{2+}$ and $[\text{S}_2\text{Mo}_{18}\text{O}_{62}]^{4-}$. Difference absorbance spectra were investigated to identify the presence of new optical transitions. Spectra of known concentrations of $[\text{Ru}(\text{bpy})_3]^{2+}$ and $[\text{S}_2\text{Mo}_{18}\text{O}_{62}]^{4-}$ were recorded separately. Difference spectra were generated by subtracting the spectra of the separate solutions from the experimental spectrum of the mixture. The

process was carried out as a function of increasing concentration of $[\text{S}_2\text{Mo}_{18}\text{O}_{62}]^{4-}$ (Figure 7).

The most striking feature of the difference spectra is the relatively intense, new absorbance feature centered around 485 nm. Interestingly, this new band corresponds closely to that observed in the excitation spectra obtained on addition of anion shown in Figure 4.

The feature is present from the first addition of anion and is present for all cation:anion ratios recorded. This new transition is consistent with ion cluster formation (eqs 1 and 2) and justifies our use of the association model for static quenching.

Raman Spectroscopy. The new visible absorbance at 485 nm was probed with resonance Raman spectroscopy to identify the origin of this optical transition. When the exciting line in Raman spectroscopy is coincident, or resonant with an optical transition, the Franck-Condon modes of the chromophore are resonantly enhanced by up to 7 orders of magnitude.¹⁷

Figure 8 a-c illustrates solid-state resonance Raman spectra, with an excitation wavelength of 488 nm, for $[(\text{C}_6\text{H}_{13})_4\text{N}]_4[\text{S}_2\text{Mo}_{18}\text{O}_{62}]$, $[\text{Ru}(\text{bpy})_3]\text{Cl}_2$, and $[\text{Ru}(\text{bpy})_3]_2[\text{S}_2\text{Mo}_{18}\text{O}_{62}]$, respectively. Both $[\text{Ru}(\text{bpy})_3]_2[\text{S}_2\text{Mo}_{18}\text{O}_{62}]$ and $[\text{Ru}(\text{bpy})_3]\text{Cl}_2$ absorb significantly at 488 nm, but $[(\text{C}_6\text{H}_{13})_4\text{N}]_4[\text{S}_2\text{Mo}_{18}\text{O}_{62}]$ does not. Consequently, Raman intensities of the latter are more than 4 orders of magnitude weaker than those of $[\text{Ru}(\text{bpy})_3]_2[\text{S}_2\text{Mo}_{18}\text{O}_{62}]$ or $[\text{Ru}(\text{bpy})_3]\text{Cl}_2$, although, for illustration, the spectra are normalized in Figure 8.

(16) Because of the assumptions inherent in this approach, we estimate the errors in these values to be up to 15%.

(17) Ferraro J.; John, R. *Introduction to Raman Spectroscopy*; Academic Press: New York, 1994.

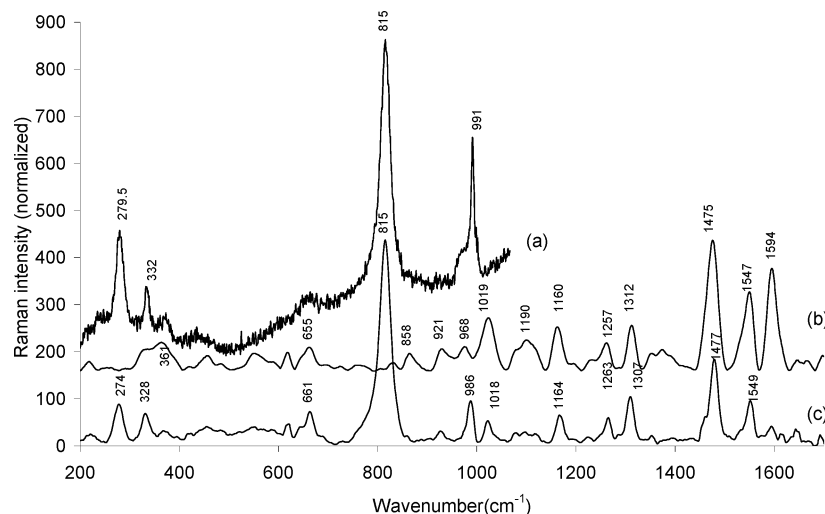


Figure 8. Resonance Raman spectrum of solids excited at 488 nm: (a) $[(\text{C}_6\text{H}_{13})_4\text{N}]_4[\text{S}_2\text{Mo}_{18}\text{O}_{62}]$; (b) $[\text{Ru}(\text{bpy})_3]\text{Cl}_2$; (c) $[\text{Ru}(\text{bpy})_3]_2[\text{S}_2\text{Mo}_{18}\text{O}_{62}]$.

It is clear that the spectrum for the 2:1 salt $[\text{Ru}(\text{bpy})_3]_2[\text{S}_2\text{Mo}_{18}\text{O}_{62}]$ contains enhanced vibrational modes associated with both $[\text{S}_2\text{Mo}_{18}\text{O}_{62}]^{4-}$ and $[\text{Ru}(\text{bpy})_3]^{2+}$. Characteristic bipyridine modes^{18,19} are enhanced at 1549, 1477, 1307, 1263, 1164, 1018, and 661 cm^{-1} , and the Ru–N stretching vibration is enhanced weakly at 378 cm^{-1} . These vibrations are observed for both $[\text{Ru}(\text{bpy})_3]_2[\text{S}_2\text{Mo}_{18}\text{O}_{62}]$ and $[\text{Ru}(\text{bpy})_3]\text{Cl}_2$ as expected since the 488 nm laser excitation lies in resonance with the $\text{Ru}(\text{d}\pi)\text{--bpy}(\pi^*)$ transition of the $[\text{Ru}(\text{bpy})_3]^{2+}$ moiety. However a striking feature is the presence of strongly enhanced modes associated with the $[\text{S}_2\text{Mo}_{18}\text{O}_{62}]^{4-}$ unit given that this anion does not absorb at 488 nm. Bands associated with Mo–O stretching modes are observed at 986 and 815 cm^{-1} ,^{20,21} and lower frequency Mo–O bending modes at 274 and 328 cm^{-1} are also enhanced. That these vibrations are so strongly enhanced with 488 nm excitation is consistent with their involvement in the underlying optical transition. Solid $[(\text{C}_6\text{H}_{13})_4\text{N}]_4[\text{S}_2\text{Mo}_{18}\text{O}_{62}]$ shows a vibration at 991 cm^{-1} which is attributed to the quaternary counterion. This signal is absent for $[\text{Ru}(\text{bpy})_3]_2[\text{S}_2\text{Mo}_{18}\text{O}_{62}]$, which may confirm the replacement of those counterions by $[\text{Ru}(\text{bpy})_3]^{2+}$.

The presence of both $[\text{S}_2\text{Mo}_{18}\text{O}_{62}]^{4-}$ and $[\text{Ru}(\text{bpy})_3]^{2+}$ vibrations in the spectrum of $[\text{Ru}(\text{bpy})_3]_2[\text{S}_2\text{Mo}_{18}\text{O}_{62}]$, Figure 8c, indicated the participation of both ions in the new optical transition observed at 485 nm. As $[\text{S}_2\text{Mo}_{18}\text{O}_{62}]^{4-}$ is fully oxidized and a strong electron acceptor and $[\text{Ru}(\text{bpy})_3]^{2+}$ may behave as electron donor, this transition is assigned tentatively to a $[\text{Ru}(\text{bpy})_3]^{2+}$ to $[\text{S}_2\text{Mo}_{18}\text{O}_{62}]^{4-}$ charge-transfer transition.

Excitations at 514 or 457.9 nm, which are post- and preresonant, respectively, with the 485 nm absorption, provided resonance Raman spectra of $[\text{Ru}(\text{bpy})_3]_2[\text{S}_2\text{Mo}_{18}\text{O}_{62}]$ ²² in which the $[\text{S}_2\text{Mo}_{18}\text{O}_{62}]^{4-}$ bands were reduced

significantly by comparison with Figure 8c. This supports the assignment of the new charge-transfer transition centered at 485 nm.²³

A number of charge transfer salts containing polyoxo-metalate anions have been reported previously.²⁴ Typically these have contained organic or ferrocenyl donating cations.²⁵ Charge-transfer transitions have been identified in these materials. However, the present system appears to be the first case in which the novel optical transition has been confirmed via resonance Raman spectroscopy and, in addition, in which the charge-transfer transition is luminescent.

Photostability. To ensure that the new optical transition observed both in the excitation and difference absorbance spectra does not arise from a photodecomposition product, the photostability of the 2:1 salt $[\text{Ru}(\text{bpy})_3]_2[\text{S}_2\text{Mo}_{18}\text{O}_{62}]$ was investigated. An acetonitrile solution (1×10^{-5} M) was irradiated for 5 h under continuous visible (>400 nm) excitation while monitoring the UV–vis spectrum. No evidence was found for photodecomposition over this period. To confirm this, a solution of $[\text{Ru}(\text{bpy})_3]\text{Cl}_2$, which was matched for absorbance intensity at 450 nm to the $[\text{Ru}(\text{bpy})_3]_2[\text{S}_2\text{Mo}_{18}\text{O}_{62}]$ solution, was photolyzed under identical conditions. The $[\text{Ru}(\text{bpy})_3]\text{Cl}_2$ underwent the anticipated facile photodecomposition, which has been reported previ-

(22) See Supporting Information.

(23) In addition to the presence of vibrational modes common to the resonance Raman spectra in Figure 8a–c, it is interesting to note the bands which are not present. Most notably, the bipyridine C–C stretch mode observed at 1594 cm^{-1} for $[\text{Ru}(\text{bpy})_3]^{2+}$ is reduced significantly in intensity in Figure 8c. Also some weaker bands, for example, at 1190 and 858 cm^{-1} , are absent in the spectrum of $[\text{Ru}(\text{bpy})_3]_2[\text{S}_2\text{Mo}_{18}\text{O}_{62}]$. The reason for the reduced intensity or absence of these bands is not clear, but since at 488 nm we are exciting primarily into what is likely to be a $\text{Ru d}\pi$ to $[\text{S}_2\text{Mo}_{18}\text{O}_{62}]^{4-}$ transition, the modes enhanced for $[\text{Ru}(\text{bpy})_3]^{2+}$ $\text{d}\pi$ to $\text{bpy } \pi^*$ transition are not necessarily enhanced here.

(24) (a) Fox, M. A.; Cardonna, E.; Gaillard, E. *J. Am. Chem. Soc.* **1987**, *109*, 6347. (b) Le Magueres, P.; Hubig, S. M.; Lindeman, S. V.; Veya, P.; Kochi, J. K. *J. Am. Chem. Soc.* **2000**, *122*, 10073. (c) Coronado, E.; Galan-Mascaros, J. R.; Gimenez-Saiz, C.; Gomez-Garcia, C. J.; Falvello, L. R.; Delhaes, P. *Inorg. Chem.* **1998**, *37*, 2183.

(25) Niu, J.-Y.; Wang, J.-P.; Chen, W.; Kennard, C. H. L.; Byriel, K. A. *J. Coord. Chem.* **2001**, *53*, 153.

(18) Coates, C. G.; Keyes, T. E.; Hughes, H. P.; Jayaweera, P. M.; McGarvey, J. J.; Vos, J. G. *J. Phys. Chem. A* **1998**, *102*, 5013.

(19) Dallinger, R. F.; Woodruff, W. H. *J. Am. Chem. Soc.* **1979**, *101*, 4391.

(20) Nakamoto, K. *Infrared and Raman Spectra of Inorganic and Coordination Compounds*, 5th ed.; Wiley: New York, 1997; Part B.

(21) Fournier, M.; Thouvenot, R.; Rocchiccioli-Deltcheff, C. *J. Chem. Soc., Faraday Trans.* **1991**, *87*, 349.

ously.²⁶ The increased photostability of the charge-transfer complex may be due to the reduced lifetime of the excited state of $[\text{Ru}(\text{bpy})_3]^{2+}$ as a consequence of adduct formation which competes with the photodecomposition reaction. Alternatively, the unstable ^3MC state responsible for photodecomposition of the $[\text{Ru}(\text{bpy})_3]^{2+}$ ion may not be accessible from the excited state of the ion cluster.

It is important to note that the 485 nm charge-transfer transition is present in both the difference absorbance spectrum and the excitation spectrum. Therefore, it must be associated with an emissive state. As the typical products of photochemical decomposition of $[\text{Ru}(\text{bpy})_3]^{2+}$ in acetonitrile, for example, $[\text{Ru}(\text{bpy})_2(\text{CH}_3\text{CN})_2]^{2+}$, are not luminescent, it is highly unlikely that the new transition is associated with such a product.

Time-Resolved Spectroscopy. As illustrated in Figure 2, the addition of $[\text{S}_2\text{Mo}_{18}\text{O}_{62}]^{4-}$ to $[\text{Ru}(\text{bpy})_3]^{2+}$ in acetonitrile solution results in a significant decrease in luminescence intensity (Figure 1). The origin of this quenching may be electron or energy transfer. In addition, as described, the photostability of the adduct would also be consistent with fast electron transfer to or from the $[\text{Ru}(\text{bpy})_3]^{2+}$ excited state.

To assess whether an electron-transfer process is feasible between $[\text{Ru}(\text{bpy})_3]^{2+}$ and $[\text{S}_2\text{Mo}_{18}\text{O}_{62}]^{4-}$, the free energy of such a process was estimated from the Rehm–Weller expression²⁷ employing the ground and excited-state redox potentials of $[\text{S}_2\text{Mo}_{18}\text{O}_{62}]^{4-}$ ²⁸ and $[\text{Ru}(\text{bpy})_3]^{2+}$, respectively.¹³ The free energy of electron transfer was estimated in this way to be -0.66 eV in a reaction in which the excited state of $[\text{Ru}(\text{bpy})_3]^{2+}$ behaves as donor and $[\text{S}_2\text{Mo}_{18}\text{O}_{62}]^{4-}$ is acceptor. This suggests such a reaction would be significantly exoergic and would appear to support electron transfer as the likely origin of the quenching mechanism. In addition, Forster energy transfer can be excluded as a possibility on the grounds of energy considerations and poor spectral overlap between the luminescent $[\text{Ru}(\text{bpy})_3]^{2+}$ state and $[\text{S}_2\text{Mo}_{18}\text{O}_{62}]^{4-}$ optical absorbance.

The quenching of $[\text{Ru}(\text{bpy})_3]^{2+}$ by $[\text{S}_2\text{Mo}_{18}\text{O}_{62}]^{4-}$ appears to be largely static in nature. However, on the basis of thermodynamic considerations, it is likely that a photoinduced electron transfer within an ion cluster may be responsible for the weak intensity of luminescence and the short lifetime. The best method of investigating the presence of photoinduced electron transfer is via time-resolved absorption spectroscopy since radical ion intermediates may be identified and followed kinetically.

Figure 9 presents time-resolved spectra for (a) $[\text{Ru}(\text{bpy})_3]_2\text{-}[\text{S}_2\text{Mo}_{18}\text{O}_{62}]$ and (b) $[\text{Ru}(\text{bpy})_3]^{2+}$ alone 20 ns after excitation in acetonitrile. Both the depletion centered at 450 nm and the absorbance at 520 nm are considerably broadened toward the UV for the ion cluster compared to $[\text{Ru}(\text{bpy})_3]^{2+}$. These

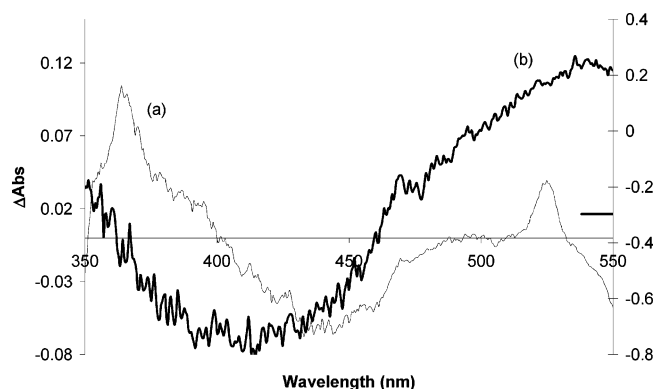


Figure 9. Transient absorption spectrum of (a) $[\text{Ru}(\text{bpy})_3]\text{Cl}_2$ and (b) $[\text{Ru}(\text{bpy})_3]_2[\text{S}_2\text{Mo}_{18}\text{O}_{62}]$ in acetonitrile excited at 355 nm 20 ns after excitation.

features in $[\text{Ru}(\text{bpy})_3]^{2+}$ are associated respectively with the depletion of the $\text{Ru}(d\pi)\text{-bpy}(\pi^*)$ MLCT and the formation of bpy^- radical states (typically at 530 nm) after charge transfer. In the present case, the depletion is still assigned to the MLCT but broadening of this feature is attributed to a contribution from the tail of the LMCT of $[\text{S}_2\text{Mo}_{18}\text{O}_{62}]^{4-}$. Spectroelectrochemistry has detected decreases in intensity on reduction of this anion.²⁹

The absorbance at 520 nm may be associated with the formation of the blue-green reduced anion $[\text{S}_2\text{Mo}_{18}\text{O}_{62}]^{5-}$ following electron transfer from $[\text{Ru}(\text{bpy})_3]^{2+}$. That this feature is not bpy^- radical is confirmed by the absence of the characteristic absorbance of this radical observed at 370 nm in the $[\text{Ru}(\text{bpy})_3]^{2+}$ spectrum. Grow-in of this feature is too fast for our instrumentation, consistent with the short-lived luminescence observed in the single photon counting measurements. This means that the photoinduced electron transfer between the $[\text{Ru}(\text{bpy})_3]^{2+}$ and $[\text{S}_2\text{Mo}_{18}\text{O}_{62}]^{4-}$ ions is also too fast for our instrumentation. The grow-in of the 450 and decay of 520 nm features follow first-order kinetics with a time constant of 80 ns in deaerated solution compared with 800 ns for $[\text{Ru}(\text{bpy})_3]^{2+}$. These kinetic processes are attributed to back electron transfer between the photooxidized $[\text{Ru}(\text{bpy})_3]^{2+}$ and the $[\text{S}_2\text{Mo}_{18}\text{O}_{62}]^{5-}$ unit. A weak luminescence was also observable in the transient spectrum of $[\text{Ru}(\text{bpy})_3]_2[\text{S}_2\text{Mo}_{18}\text{O}_{62}]$ centered at 600 nm with a lifetime of 800 ns. This was attributable to residual free $[\text{Ru}(\text{bpy})_3]^{2+}$ in solution. The detailed kinetics of this system are currently undergoing further study and will be presented at a later date.

Conclusions

In this paper we present a photophysical and spectroscopic study of cluster ion formation between $[\text{Ru}(\text{bpy})_3]^{2+}$ and $[\text{S}_2\text{Mo}_{18}\text{O}_{62}]^{4-}$. Comparison of steady-state and time-resolved luminescence methods indicate that quenching of $[\text{Ru}(\text{bpy})_3]^{2+}$ by $[\text{S}_2\text{Mo}_{18}\text{O}_{62}]^{4-}$ occurs via a purely static mechanism. Steady-state spectra indicate efficient quenching of the $^3\text{MLCT}$ of $[\text{Ru}(\text{bpy})_3]^{2+}$ by $[\text{S}_2\text{Mo}_{18}\text{O}_{62}]^{4-}$, but time-resolved luminescence spectra show that the lifetime of $[\text{Ru}(\text{bpy})_3]^{2+}$ is not influenced by the addition of the anion. Complex formation is inhibited in high ionic strength

(26) Durham, B.; Caspar, J. V.; Nagel, J. K.; Meyer, T. J. *J. Am. Chem. Soc.* **1982**, *104*, 4803.

(27) Rehm–Weller expression: ΔG (eV) = $[E(\text{D}^+/\text{D}) - E(\text{A}/\text{A}^-)] - E_{0-0}$, where $E(\text{D}^+/\text{D})$ and $E(\text{A}/\text{A}^-)$ are the oxidation and reduction potentials of donor and acceptor sites, respectively, and E_{0-0} is the zero-zero spectroscopic energy calculated from the 77 K emission spectrum.

(28) Bond, A. M.; Vu, T.; Wedd, A. G. *J. Electroanal. Chem.* **2000**, *494*, 96.

(29) Vu, T. Ph.D. Thesis, Monash University, Victoria, Australia, 1999.

solutions. The complexes are completely dissociated in 0.1 M LiClO_4 or $(\text{TEA})\text{BF}_4$ solutions, suggesting the $[\text{S}_2\text{Mo}_{18}\text{O}_{62}]^{4-}$ – $[\text{Ru}(\text{bpy})_3]^{2+}$ interaction is purely electrostatic in nature. Spectroscopic data suggest that the cation and anion interact in 1:1 and 2:1 $[\text{Ru}(\text{bpy})_3]^{2+}:[\text{S}_2\text{Mo}_{18}\text{O}_{62}]^{4-}$ ratios. Formation of these new cluster species results in significant quenching of the $[\text{Ru}(\text{bpy})_3]^{2+}$ excited state. However, a weak, short-lived luminescence is observed from the new adduct species. The origin of this new luminescence is confirmed via excitation and difference absorbance spectroscopy to be a new optical transition, associated with the ion cluster, centered 485 nm. Resonance Raman spectroscopy was employed to assign this transition as a $[\text{Ru}(\text{bpy})_3]^{2+}$ to $[\text{S}_2\text{Mo}_{18}\text{O}_{62}]^{4-}$ charge transfer. This is the first report of a luminescent charge-transfer state involving $[\text{Ru}(\text{bpy})_3]^{2+}$ in which the luminescence does not originate solely from this species.

Excited-state electron transfer between $[\text{Ru}(\text{bpy})_3]^{2+}$ and $[\text{S}_2\text{Mo}_{18}\text{O}_{62}]^{4-}$ seems likely to be the origin of the weak short-lived emission observed in the adducts. This is confirmed

in preliminary transient spectroscopy which shows evidence for the formation of a short-lived charge-separated $[\text{Ru}(\text{III})-(\text{bpy})_3]^{3+}$ – $[\text{S}_2\text{Mo}_{18}\text{O}_{62}]^{5-}$ species.

We are currently investigating the detailed kinetics of the excited-state electron transfer and charge recombination processes in this ion cluster.

Acknowledgment. The authors gratefully acknowledge the Australian Research Council for funding under Grant A00103315. T.E.K., E.G., and L.G. gratefully acknowledge Enterprise Ireland under Grants ST/2000/356 and SC/99/236. Part of this work was conducted at FOCAS, DIT, which is funded under the National Development Plan 2000 to 2006 with assistance from the European Regional Development Fund. T.E.K. gratefully acknowledges Johnson Matthey for the generous loan of RuCl_3 .

Supporting Information Available: Raman spectra of solid $[\text{Ru}(\text{bpy})_3]_2[\text{S}_2\text{Mo}_{18}\text{O}_{62}]$ excited at 457.9 and 514 nm. This material is available free of charge via the Internet at <http://pubs.acs.org>.

IC0206802